

## Structural properties and energetics of diffuse $87\text{Rb}$ clusters in three-dimension

Pankaj Kumar Debnath, Barnali Chakrabarti, Tapan Kumar Das, and Sylvio Canuto

Citation: *The Journal of Chemical Physics* **137**, 014301 (2012); doi: 10.1063/1.4730972

View online: <http://dx.doi.org/10.1063/1.4730972>

View Table of Contents: <http://scitation.aip.org/content/aip/journal/jcp/137/1?ver=pdfcov>

Published by the [AIP Publishing](#)

---

### Articles you may be interested in

[A theoretical study of  \$\text{Ne}\_3\$  using hyperspherical coordinates and a slow variable discretization approach](#)  
*J. Chem. Phys.* **135**, 134312 (2011); 10.1063/1.3645183

[Higher order two- and three-body dispersion coefficients for alkali isoelectronic sequences by a variationally stable procedure](#)  
*J. Chem. Phys.* **134**, 144110 (2011); 10.1063/1.3577967

[Pair-correlation properties and momentum distribution of finite number of interacting trapped bosons in three dimensions](#)  
*J. Chem. Phys.* **133**, 104502 (2010); 10.1063/1.3488650

[Electronically excited rubidium atom in a helium cluster or film](#)  
*J. Chem. Phys.* **129**, 184308 (2008); 10.1063/1.3009279

[Monte Carlo hyperspherical description of helium cluster excited states](#)  
*J. Chem. Phys.* **112**, 8053 (2000); 10.1063/1.481404

---



**AIP** | Journal of  
Applied Physics

*Journal of Applied Physics* is pleased to  
announce **André Anders** as its new Editor-in-Chief

# Structural properties and energetics of diffuse $^{87}\text{Rb}$ clusters in three-dimension

Pankaj Kumar Debnath,<sup>1</sup> Barnali Chakrabarti,<sup>2,a)</sup> Tapan Kumar Das,<sup>3</sup> and Sylvio Canuto<sup>2</sup>

<sup>1</sup>*Santoshpur Sri Gouranga Vidyapith (H.S.), P.O.-Kulitapara, Howrah 711312, India*

<sup>2</sup>*Instituto de Fisica, Universidade de São Paulo, CP 66318, 05315-970 São Paulo, SP, Brazil*

<sup>3</sup>*Department of Physics, University of Calcutta, 92 A.P.C. Road, Kolkata 700009, India*

(Received 22 December 2011; accepted 11 June 2012; published online 2 July 2012)

A correlated two-body basis function is used to describe the three-dimensional bosonic clusters interacting via two-body van der Waals potential. We calculate the ground state and the zero orbital angular momentum excited states for  $\text{Rb}_N$  clusters with up to  $N = 40$ . We solve the many-particle Schrödinger equation by potential harmonics expansion method, which keeps all possible two-body correlations in the calculation and determines the lowest effective many-body potential. We study energetics and structural properties for such diffuse clusters both at dimer and tuned scattering length. The motivation of the present study is to investigate the possibility of formation of  $N$ -body clusters interacting through the van der Waals interaction. We also compare the system with the well studied He, Ne, and Ar clusters. We also calculate correlation properties and observe the generalised Tjon line for large cluster. We test the validity of the shape-independent potential in the calculation of the ground state energy of such diffuse cluster. These are the first such calculations reported for Rb clusters. © 2012 American Institute of Physics. [<http://dx.doi.org/10.1063/1.4730972>]

## I. INTRODUCTION

Weakly bound few-body systems are the subject of great interest since a long time back and it is still an ongoing issue in atomic, nuclear, and condensed matter physics.<sup>1-5</sup> For more than a decade, such diffuse systems have generated a new interest in the context of ultracold atomic physics and the Bose-Einstein condensation (BEC). By using selective laser pumping, it is easy to prepare a dilute atomic vapor in a particular hyperfine state. Alkali atoms, specially Rb atoms, are good candidates for laser manipulation and to observe BEC. The external magnetic field provides the trapping, which is required for producing BEC. It is reached when all the atoms condense to the lowest energy level in the external trap.<sup>6</sup> The external trapping potential is generally described by  $V_{\text{trap}} = \frac{1}{2}m\omega^2 r^2$ , where  $\omega$  is the trap frequency. As the interatomic potential is very weak compared to the external trapping potential, the system is treated as a weakly interacting Bose gas. Furthermore, the system is very dilute and the interatomic interaction is fairly well represented by the zero-range potential. Consequently, the system can be described by the Gross Pitaevskii (GP) mean-field equation.<sup>6</sup>

In the present study, we are interested in the bound  $N$ -body clusters of Rb atoms in the absence of an external trap. In the GP equation, the strength of the zero-range interaction is given by  $g = \frac{4\pi\hbar^2 a_s}{m}$ , where  $m$  is the atomic mass and  $a_s$  is the  $s$ -wave scattering length. Thus, a positive value of  $a_s$  corresponds to a repulsive BEC while its negative value corresponds to an attractive BEC. In this case, the long-range attractive part of the realistic interatomic interaction is com-

pletely neglected. For the attractive contact interaction, the singularity at the center of the condensate is disregarded in the GP equation approach. This is justified only in the presence of an external trap, as the trap energy is quite high compared with the interaction energy in the metastable region of the zero-temperature BEC. The attractive contact interaction without a trap leads to a catastrophic collapse and cannot produce stable clusters. In the absence of a trap, binding is provided by the two-body van der Waals (vdW) potential, having a short range repulsive core below a cut off radius and a  $-\frac{C_6}{r^6}$  tail, which represents the long-range attractive part.<sup>7</sup> We wish to examine the stability of such coherent clusters both at the dimer and the tuned scattering length. Use of Feshbach resonance by manipulation of an applied magnetic field makes it possible to tune  $a_s$  to any value, including sign.<sup>8</sup> The unmanipulated scattering length, which gives rise to an atomic dimer, is referred to as the dimer scattering length. This opens the experimental avenue for playing with the effective interaction. The strength parameter  $C_6$  of the vdW potential is known for Rb atoms and  $a_s$  can be obtained by solving the zero-energy two-body Schrödinger equation with the two-body van der Waals potential.<sup>7</sup> We adjust the hard core radius such that  $a_s$  has the desired value. Thus, utilizing the Feshbach resonance, the effective interaction between two atoms can be changed essentially to any value as desired and it facilitates the creation of large weakly bound clusters. Our present study is important in the context of recent experiments on weakly bound molecules created by Feshbach resonance in an ultra cold Bose gas.<sup>9-12</sup> We study the stability of  $N$ -body clusters by changing the scattering length from its dimer value. We observe a strong dominating role of the attractive part of the interaction over the repulsive part. The study of structural properties and the calculation of a number of excited states have also been performed.

<sup>a)</sup>Permanent address: Department of Physics, Lady Brabourne College, P1/2 Surawardi Avenue, Kolkata 700017, India. E-mail: chakb@rediffmail.com.

The solution of such many-body Schrödinger equation both for the ground and the excited states is also a challenging problem. Although adiabatic hyperspherical technique has been extensively used in three-body systems,<sup>13</sup> its application to many-particle systems is restricted. The main difficulty comes in the determination of the many-body effective potential, which is calculated by the diagonalization of the potential matrix. The matrix elements involve integrals over  $(3N - 1)$  hyperangles and due to large degeneracy of the hyperspherical harmonics (HH) basis, the calculation of the potential matrix becomes essentially impossible when  $N > 3$ . Large degeneracy in the HH basis arises due to the presence of all possible many-body correlations. But for the diffuse systems, one can safely ignore the effect of three and higher-body correlations keeping only the two-body correlations in the calculation. The physical picture is the following: when two bosons interact, the remaining  $(N - 2)$  bosons are inert spectators and we can freeze all the degrees of freedom coming from these atoms. This picture is valid for all interacting pairs, justifying the choice a subset of the full HH basis, which incorporates only two-body correlations. This new basis is called potential harmonics (PH) basis. Recently, we have extensively applied this basis function to describe the dilute BEC and have successfully reproduced many experimental observations.<sup>14,15</sup> We have also studied small He clusters by utilizing the PH basis.<sup>16</sup> However, Rb clusters are quite different from the He clusters. In the small He clusters, the negative interaction energy is quite large compared to the ground state energy, due to a large cancellation in the latter with the large kinetic energy (KE) arising from the small mass of He atoms. Hence, the system is highly correlated at short interatomic separations. We have observed in our earlier calculation that the standard PH basis function is not sufficient to reproduce the energetics of such correlated system.<sup>16</sup> So, in our previous calculation for the He clusters, we multiplied the PH basis function with a suitable two-body *short-range correlation function*, which is determined directly from the zero-energy solution of the two-body Schrödinger equation.<sup>17</sup> We called this basis set as correlated PH or CPH basis. However, due to smaller KE, arising from the larger mass of Rb atoms interacting via van der Waals potential, negative interaction energy is comparable with the negative ground state energy as the interaction energy does not cancel with KE largely. So, the system of Rb atoms is strongly bound but is less correlated at short interatomic separations, whereas He clusters are less bound but have strong short-range correlations. So, for the present study, we utilize the PH basis without additional short-range correlation functions for the calculation of several energetics and structural properties for the diffuse clusters. Successful application of this basis for the van der Waals clusters justifies our approach. Since the numerical complications will be significantly reduced in this approach, we can handle quite a large number of bosons in the ensemble, bound by the van der Waals force. In our present study, we treat clusters containing up to  $N = 40$  atoms.

Thus, the present study is important for several reasons. First: the recent experiments on weakly bound clusters, created using the Feshbach resonance in ultra cold Bose gas, motivate us to study larger weakly bound clusters. Second: the

standard PH basis (with standard long-range two-body correlations, but without additional short-range correlation functions) adopted for the present study is well justified for such heavier diffuse clusters. This makes it possible to study large clusters with varying atom-atom scattering lengths. Although the structural properties of Ne and Ar clusters containing  $N = 3 - 6$  atoms are well studied,<sup>18</sup> the Rb-atom clusters have not been studied yet. Thus, our interest in this paper is the detailed description of weakly bound clusters with different scattering lengths, to study the stability of the clusters, their energetics and structural properties. We also test the validity of the shape-independent approximation, i.e., the effect of different strength parameter  $C_6$  on the ground state energy. We also calculate the decay rate by three-body recombination, which plays an important role in the stability of deeply bound cluster. In the process, we are also interested to see the usefulness of the PH basis and its limitation in the description of the van der Waals clusters.

The paper is organized as follows. Section II briefly describes the many-body technique, which takes care of the two-body correlation and interatomic interaction. Section III presents results for the various structural properties of the diffuse clusters. Section IV concludes with a summary.

## II. POTENTIAL HARMONICS BASIS AND THE COUPLED DIFFERENTIAL EQUATION FOR $N$ -BODY CLUSTERS

As mentioned in the introduction, we adopt the potential harmonics expansion method (PHEM) for our calculation. This technique is already well documented, hence only a brief outline is provided here. The interested reader can find details in Refs. 14 and 19.

The relative motion of the  $N$ -body system interacting through mutual two-body forces ( $V$ ) can be expressed in terms of  $\vec{N} = N - 1$  Jacobi vectors  $\{\vec{\zeta}_i, i = 1, \vec{N}\}$  (Ref. 20)

$$\left[ -\frac{\hbar^2}{m} \sum_{i=1}^{\vec{N}} \nabla_{\zeta_i}^2 + V(\vec{\zeta}_1, \dots, \vec{\zeta}_{\vec{N}}) - E \right] \Psi(\vec{\zeta}_1, \dots, \vec{\zeta}_{\vec{N}}) = 0. \quad (1)$$

For a full *ab initio* treatment, the many-body wave function can be expanded in the complete basis of hyperspherical harmonics.<sup>20</sup> As explained earlier, it becomes intractable for  $N > 3$ . However, for a dilute system like the Rb-cluster, only two-body correlations are relevant. Then  $\Psi$  can be decomposed in Faddeev components

$$\Psi(\vec{x}) = \sum_{i,j>i}^N \psi_{ij}(\vec{x}), \quad (\vec{x} \equiv \{\vec{x}_1, \dots, \vec{x}_N\}). \quad (2)$$

Since only two-body correlations and two-body interactions are relevant for the diffuse cluster,  $\psi_{ij}$  is a function of two-body separation vector,  $\vec{r}_{ij} = \vec{x}_i - \vec{x}_j$  only, besides the global length called hyper-radius ( $r$ ).  $\psi_{ij}$  is symmetric under  $P_{ij}$  for bosonic atoms and satisfies the Faddeev equation

$$(T - E)\psi_{ij}(\vec{x}) = -V(\vec{r}_{ij}) \sum_{k,l>k} \psi_{kl}(\vec{x}), \quad (3)$$

$T$  being the total kinetic energy. Since  $\psi_{ij}$  is a function of  $\vec{r}_{ij}$  and  $r$  only, it is expanded in the set of potential harmonics [subset of HH sufficient for the expansion of  $V(\vec{r}_{ij})$ ] appropriate for the  $(ij)$  partition<sup>19</sup>

$$\psi_{ij} = r^{-\frac{3\bar{N}-1}{2}} \sum_K \mathcal{P}_{2K+l}^{lm}(\Omega_N^{(ij)}) u_K^l(r). \quad (4)$$

Substituting in Eq. (3) and projecting on a particular PH, a set of coupled differential equations (CDE) for the partial wave  $U_{Kl}(r)$  is obtained

$$\left[ -\frac{\hbar^2}{m} \frac{d^2}{dr^2} + \frac{\hbar^2}{mr^2} \{ \bar{\mathcal{L}}(\bar{\mathcal{L}} + 1) + 4K(K + \alpha + \beta + 1) \} + E \right] U_{Kl}(r) + \sum_{K'} f_{Kl} V_{KK'}(r) f_{K'l} U_{K'l}(r) = 0, \quad (5)$$

where  $U_{Kl}(r) = f_{Kl} u_K^l(r)$ ,  $\bar{\mathcal{L}} = l + \frac{3\bar{N}-3}{2}$ ,  $\alpha = \frac{3\bar{N}-5}{2}$ ,  $\beta = l + \frac{1}{2}$ ,  $l$  being the orbital angular momentum contributed by the interacting pair, and  $K$  is the hyperangular momentum quantum number. The constant  $f_{Kl}$  is the overlap of the PH for interacting partition with the sum of PHs corresponding to *all* partitions.<sup>19,21</sup> The potential matrix element  $V_{KK'}(r)$  is given by

$$V_{KK'}(r) = \int \mathcal{P}_{2K+l}^{lm*}(\Omega_N^{ij}) V(r_{ij}) \mathcal{P}_{2K'+l}^{lm}(\Omega_N^{ij}) d\Omega_N^{ij}. \quad (6)$$

The PH basis has recently been successfully applied to <sup>4</sup>He trimer and clusters with a maximum of nine He atoms.<sup>16</sup> In that study, we introduced a short-range correlation function in the expansion basis, which takes into account the strong repulsion of He–He potential, seen by pairs coming close enough due to their large KE. This function successfully manifests the strong short-range two-body correlation. By contrast, due to the larger mass, Rb atoms have smaller KE and the interacting atoms do not come close enough to feel the strong repulsive core. Hence, the PH basis without a short-range correlation, is quite accurate for large Rb clusters.

### III. RESULTS

#### A. Choice of interaction and calculation of many-body effective potential

As an interaction potential, we choose the van der Waals potential with a hard core of radius  $r_c$ , *viz.*,  $V(r_{ij}) = \infty$  for  $r_{ij} \leq r_c$  and  $-\frac{C_6}{r_{ij}^6}$  for  $r_{ij} > r_c$ . For Rb atoms, the value of  $C_6$  parameter is obtained from Ref. 7 and has the value 2803 eV Å<sup>6</sup>. For a given finite range two-body potential,  $a_s$  can be obtained by solving the zero-energy two-body Schrödinger equation for the wavefunction  $\eta(r_{ij})$  (Ref. 7)

$$-\frac{\hbar^2}{m} \frac{1}{r_{ij}^2} \frac{d}{dr_{ij}} \left( r_{ij}^2 \frac{d\eta(r_{ij})}{dr_{ij}} \right) + V(r_{ij})\eta(r_{ij}) = 0. \quad (7)$$

The asymptotic form of  $\eta(r_{ij})$  is  $C(1 - \frac{a_s}{r_{ij}})$ ,  $C$  being a normalization constant. We adjust the hard core radius  $r_c$  in the two-

body equation to correctly obtain the desired  $a_s$ .<sup>7,17</sup> The solution of two-body equation shows that the value of  $a_s$  changes from negative to positive, passing through an infinite discontinuity as  $a_s$  decreases (see Fig. 1 of Ref. 17). At each discontinuity, one extra node in the two-body wave function appears, which corresponds to one extra two-body bound state. Thus, a tiny increase in  $r_c$  across the infinite discontinuity causes  $a_s$  to jump from a very large positive value to a very large negative value. In two-body solution, we tune  $r_c$  such that it corresponds to single node in the two-body wave function and gives the desired  $a_s$ . Calculated values of  $r_c$  are 14.7532 Å, 15.1800 Å, and 15.79526 Å for  $a_s = 10$  Bohr, 100 Bohr, and 2000 Bohr, respectively. The two-body interaction is chosen as the van der Waals potential with these sets of values of  $(C_6, r_c)$ . As mentioned earlier, we include  $\eta(r_{ij})$  in the PH expansion basis, Eq. (4), as a short-range correlation function (SRCF) in the case of He cluster. However, it was also mentioned that due to a small kinetic energy in Rb clusters, the Rb atoms do not come too close to each other and therefore, no additional SRCF is needed. The effect of a change in  $a_s$  goes directly into the two-body interaction through the changed  $r_c$ . Note that the potential is deepest and changes rapidly just outside  $r_c$ . We next solve the set of CDEs, Eq. (5), by hyperspherical adiabatic approximation (HAA),<sup>22</sup> where hyper-radial motion is assumed to be slow compared to the hyperangular motion. This is intuitively justified, since the hyper-radial motion corresponds to the breathing mode of the entire system. A solution of the hyperangular motion is obtained by diagonalizing the potential matrix including the diagonal hypercentrifugal repulsion [second term of Eq. (5)] for a fixed value of  $r$ . The lowest eigenvalue,  $\omega_0(r)$ , provides the effective potential in which the hyper-radial motion takes place.<sup>22</sup> The CDE, Eq. (5), is then decoupled approximately into a single uncoupled differential equation

$$\left[ -\frac{\hbar^2}{m} \frac{d^2}{dr^2} + \omega_0(r) + \sum_{K=0}^{K_{max}} \left| \frac{d\chi_{K0}(r)}{dr} \right|^2 - E \right] \zeta_0(r) = 0. \quad (8)$$

This is solved, subject to appropriate boundary conditions on  $\zeta_0(r)$  to obtain the energy and wave function approximately. The third term in Eq. (8) is a correction to the lowest order HAA approximation.  $\chi_{K0}(r)$  is the  $K$ th component of the column eigenvector of the potential plus hypercentrifugal matrix, corresponding to the lowest eigenvalue  $\omega_0(r)$ . This is called uncoupled adiabatic approximation (UAA), whereas disregarding the third term corresponds to the extreme adiabatic approximation (EAA). For the present calculation, we employ EAA, which is already established as a good approximation in different nuclear and atomic problems.<sup>23</sup> By using HAA, the multidimensional problem is essentially reduced to an effective one-dimensional problem. Besides reducing computations greatly, it gives an effective potential, which provides both qualitative visualization and quantitative information about the system under study. Even though the computations are greatly simplified, the HAA has been shown to be surprisingly accurate for nuclear, atomic, and molecular systems.<sup>23</sup> Using the effective potential  $\omega_0(r)$ , we can monitor the structural properties of the system as a function of

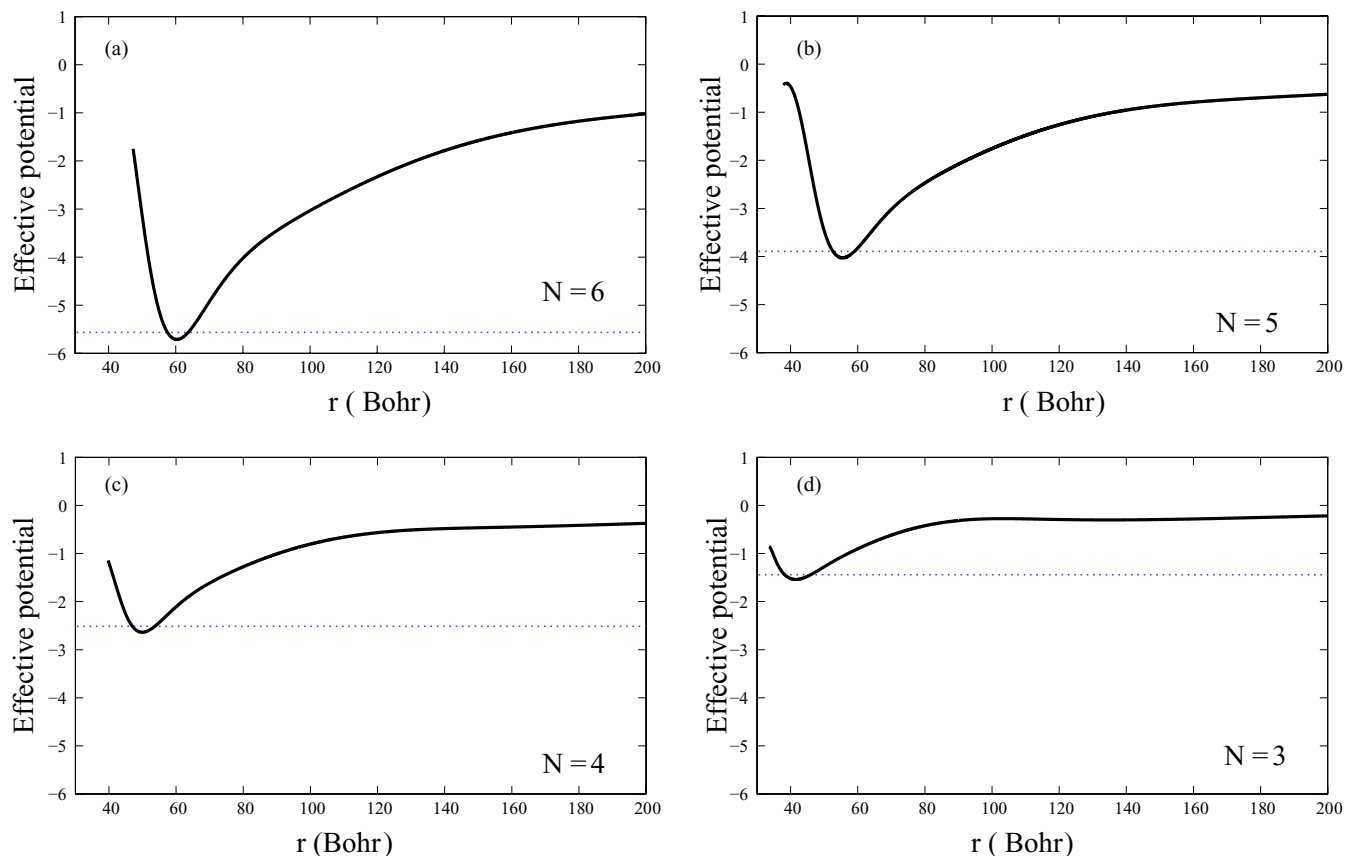


FIG. 1. Plot of effective potential (in  $\text{cm}^{-1}$ ) as a function of hyper-radius,  $r$ , at dimer scattering length for  $N = 6, 5, 4$ , and  $3$  atoms. Blue line corresponds to ground state energy.

hyper-radius. We can also interpret the size of the system and correlation properties. The separation into the hyper-radial and the hyperangular motion also facilitates the approximate calculation of excited states. In this work, we select the  $l = 0$  states and truncate the PH basis to a maximum value  $K = K_{max}$ , which provides the desired convergence.

## B. Energetics of $N$ -body Rb clusters with $N \leq 40$ atoms at dimer scattering length

This section presents the energetics of  $N$ -body Rb clusters at Rb–Rb scattering length  $a_s = 100$  Bohr, which is the natural Rb–Rb scattering length, referred to as the *dimer* scattering length. We are particularly interested in the study of stable bound clusters due to the van der Waals interaction of the atom-pairs. The long-range attractive tail of the van der Waals interaction plays an important role in the formation of bound clusters. In Fig. 1, we plot the many-body effective potential,  $\omega_0(r)$ , as a function of hyper-radius  $r$ , for consecutive atom numbers  $N = 3 - 6$ . In Fig. 2, we plot  $\omega_0(r)$  for  $N = 10, 20, 30$ , and  $40$ . We point out several features of these potentials and compare them with the earlier results of He and other rare gas clusters. With increase in atom number, the minimum of the lowest eigenpotential  $\omega_{0m}$  decreases and the position of the minimum  $r_m$  gradually increases. Their numerical values are presented in Table I. Figures 1 and 2 clearly show that with increase in the number of atoms in the cluster, it becomes more bound and the size of the cluster increases rapidly. The

size of the many-body system in three-dimensional physical space is roughly  $\sqrt{\frac{1}{2N}}$  of the hyper-radial extent.<sup>19</sup> Taking this into account, one notices that the size of Rb cluster increases slowly with  $N$ , which characterizes an increasing diffuseness of the system with  $N$ . It is in perfect agreement with intuition. The stability of diffuse Rb cluster arises solely due to van der Waals attractive interaction coming from  $\frac{N(N-1)}{2}$  interacting pairs. We observe an important difference in the nature of effective potential compared with that for He, Ne, and Ar clusters. Unlike the rare gas clusters, the threshold (asymptotic value) of the effective potential curve for a cluster

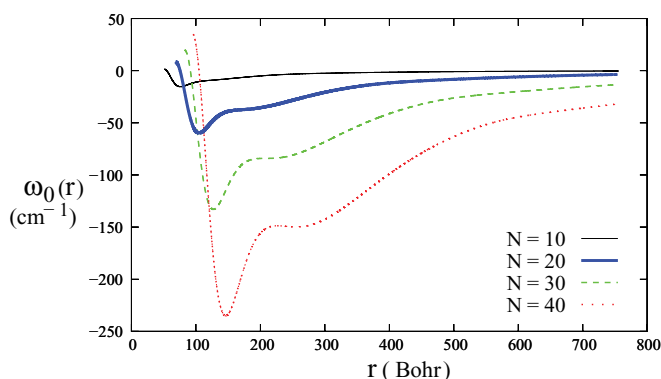


FIG. 2. Plot of effective potential,  $\omega_0(r)$ , as a function of hyper-radius,  $r$ , at the dimer scattering length for indicated cluster sizes.

TABLE I. Position ( $r_m$ ) and value ( $\omega_{0m}$ ) of the minimum of lowest eigenpotential  $\omega_0(r)$  for different  $\text{Rb}_N$  clusters. Length and energy are in units of Bohr and  $\text{cm}^{-1}$ , respectively.

N	$r_m$	$\omega_{0m}$
3	41.536	-1.532
4	49.927	-2.580
5	55.482	-4.032
6	60.320	-5.711
7	64.704	-7.689
8	68.748	-9.959
9	72.528	-12.519
10	76.080	-15.369
20	104.917	-59.774
30	127.216	-133.045
40	146.170	-235.174

having  $N$  atoms is *not* identical to the ground state energy of  $(N - 1)$  atom cluster for Rb system. Thus, we cannot conclude that the ground state energy of the  $(N - 1)$ -body Rb cluster and the potential energy of an Rb atom incident on the  $(N - 1)$ -body cluster to be equal to the ground state energy of the  $N$ -body cluster. This observation is in sharp contrast with the observations made earlier in the study of He, Ne, and Ar clusters with atom numbers  $N = 3 - 6$  (Ref. 18). Thus, in Rb cluster, we cannot identify that  $N$  atom cluster fragments into an  $(N - 1)$  atom cluster and an atom. Further support comes from the following observation. In  $\text{Ne}_N$  clusters, increasing  $N$  from 3 to 4, the ground state energy ( $E_0$ ) increases by  $-43.17 \text{ cm}^{-1}$  (Ref. 18). Also in  $\text{Ar}_N$  clusters, increasing  $N$  as before,  $E_0$  increases by  $-212.82 \text{ cm}^{-1}$ . Whereas for the diffuse Rb system, we have observed that increasing  $N$  as before,  $E_0$  changes only by  $-1.11 \text{ cm}^{-1}$ . This picture is true also for other values of  $N$ . In Table II, we summarize

TABLE II. Comparison of ground state energetics for  $\text{Rb}_N$  ( $N = 3$  to 40) cluster and for  $\text{He}_N$  ( $N = 3$  to 9) cluster.  $E_0$  is the ground state energy,  $\frac{E_0}{N}$  is the ground state energy per particle, and  $\langle V \rangle$  is the expectation value of the interaction energy. All energies are in  $\text{cm}^{-1}$ .

Atom	N	$E_0$	$\frac{E_0}{N}$	$\langle V \rangle$	$E_0$ by LJ potential
Rb	3	-1.4081	-0.46933	-1.5093	-1.41030
	4	-2.5135	-0.6284	-2.5877	-2.52165
	5	-3.8932	-0.7786	-3.9754	-3.90558
	6	-5.5651	-0.9275	-5.6589	-5.58290
	7	-7.5323	-1.0760	-7.6332	-7.55626
	8	-9.7908	-1.2238	-9.9022	-9.82172
	9	-12.3401	-1.3711	-12.4622	-12.37820
	10	-15.1802	-1.5180	-15.3124	-15.22835
	20	-59.4970	-2.9748	-59.7289	
	30	-132.7029	-4.4234	-133.0276	
40	-234.4554	-5.8613	-235.1880		
$\text{He}^a$	3	-0.0872	-0.029	-1.26	
	4	-0.388	-0.0970	-3.78	
	5	-0.905	-0.1810	-6.32	
	6	-1.605	-0.2675	-9.74	
	7	-2.330	-0.3328	-13.70	
	8	-2.896	-0.3618	-18.00	
	9	-3.097	-0.3441	-22.60	

<sup>a</sup>Reference 16.

energetics of Rb clusters for different cluster sizes ( $N$ ). For comparison, we also present energetics calculated for small He clusters with correlated PH basis,<sup>16</sup> which are comparable with the diffusion quantum Monte Carlo (DMC) results.<sup>25</sup> Comparing the ground state energies, one finds that Rb clusters are strongly bound compared to He clusters. Due to the small mass of He atom, kinetic energy of  $\text{He}_N$  clusters is large and cancels largely with the large negative interaction energy  $\langle V \rangle$ , making the binding energy of the system small. Large KE permits a pair of atom to come close enough, invoking a strong short-range correlation. On the other hand, due to the heavier mass of the Rb atom, KE of  $\text{Rb}_N$  clusters is small, while  $\langle V \rangle$  is large. Hence, total energy is large negative, making the system tightly bound but with no short range correlation. Thus, our PH method without a short-range correlation works well, while the CPH method was necessary for the He clusters.<sup>16</sup> For the completeness of our observation, we also present results for ground state energy using Lennard-Jones (LJ) potential, viz.,  $V(r_{ij}) = \frac{C_{12}}{r_{ij}^{12}} - \frac{C_6}{r_{ij}^6}$  for few number of clusters. For the LJ potential, we keep the same value of  $C_6$  as before and adjust the value of  $C_{12}$  to get the same dimer scattering length. The results are in agreement with van der Waals potential for small cluster. However, deviation in the ground state energy increases with increase in cluster size. For the comparison of compactness of He and Rb clusters, we plot  $\Delta E = E^{(N+1)} - E^{(N)}$  as a function of  $N$  in Fig. 3, and in Fig. 4, we plot the average size  $R_{av}$  (in the hyper-radial space) of the clusters as a function of cluster size  $N$ . In Fig. 3, we observe that  $\Delta E$  for  $\text{He}_N$  cluster decreases smoothly and slowly with increase in  $N$ , which indicates that He cluster is correlated and compact. Figure 4 shows that the average size of the  $\text{He}_N$  cluster also slowly increases with  $N$ . It signifies the saturation in density and predicts the liquid-drop behaviour in He system with large  $N$ . Whereas in  $\text{Rb}_N$  cluster,  $\Delta E$  sharply becomes more negative and the average size sharply increases with the increase in  $N$ . It indicates that Rb cluster is dilute and diffuse, with no apparent saturation in density as observed in the  $\text{He}_N$  cluster. Further support of this conclusion comes from the following. The physical size of the system is given by  $R_{av}/\sqrt{2N}$ <sup>19</sup> and we find that this quantity increases faster with  $N$ , than a liquid drop behavior would suggest, for the Rb clusters. Thus, the Rb cluster remains

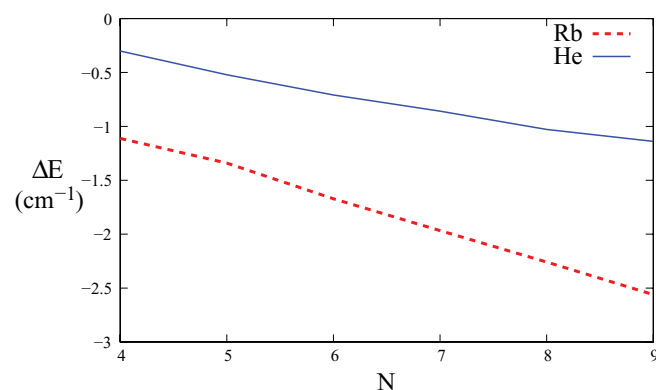


FIG. 3. Plot of the difference in two consecutive cluster energies,  $\Delta E = E^{(N+1)} - E^{(N)}$ , as a function of cluster size  $N$ .

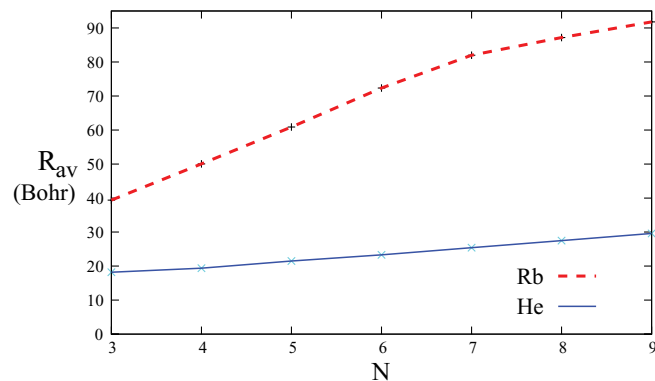


FIG. 4. Plot of the average size of cluster,  $R_{av}$ , as a function of cluster size  $N$  for Rb and He clusters.

diffused even with increase of  $N$  although it is still tightly bound. On the other hand, the rare gas clusters become increasingly compact, since their physical size decreases rapidly with  $N$ .

Next we calculate the energy  $E_n$  with  $n > 0$  of several  $L = 0$  bound states of Rb clusters using the one-dimensional effective potential in the hyper-radial coordinate. For comparison with available results of  $\text{He}_N$  clusters, we summarize the values of  $E_1$ ,  $E_2$ , and  $E_3$  for different cluster sizes  $N$  of He and Rb clusters in Table III. With increase in  $N$ , all these states become more bound. One notices that all the higher excited states of Rb clusters are very strongly bound compared to the small He clusters. In the earlier study of Ne and Ar clusters with  $N = 3 - 6$  atoms,<sup>18</sup> a similar trend was observed although large quantitative difference exists. This difference is attributed to the compactness of rare gas clusters. In this context, it is very important to study the effect of shape-dependent potential in the calculation of ground state energy. In our earlier study of interacting trapped bosons, it is observed that the ground state energy is dependent on the actual shape of two-body potential.<sup>24</sup> In our present study, we choose several  $C_6$  values (both above and below the actual  $C_6$  parameter of dimer). The calculated ground state energies are plotted for different cluster size in Fig 5. For all the  $C_6$  parameters, we appropriately tune  $r_c$  such that due to variation of ( $C_6$ ,  $r_c$ ),

TABLE III. Comparison of first few excited state energies of He and Rb clusters.  $E_1$ ,  $E_2$ ,  $E_3$  are the energies of first, second, and third excited states, respectively. The energies are in  $\text{cm}^{-1}$ .

$N$	$E_1$		$E_2$		$E_3$	
	Rb	He	Rb	He	Rb	He
3	-1.2291	-0.00152	-0.9827		-0.7269	
4	-2.2707	-0.0922	-2.0105		-1.7164	
5	-3.6283	-0.418	-3.3484	-0.208	-3.0305	-0.048
6	-5.2696	-0.894	-4.9459	-0.453	-4.5766	-0.266
7	-7.2245	-1.483	-6.9126	-0.875	-6.5713	-0.466
8	-9.4624	-1.982	-9.1465	-1.287	-8.8431	-0.780
9	-11.989	-2.189	-11.648	-1.480	-11.311	-0.946
10	-14.8074		-14.4436		-14.0910	
20	-58.9473		-58.4014		-57.8569	
30	-132.019		-131.337		-130.6607	
40	-233.1283		-231.7011		-230.2162	

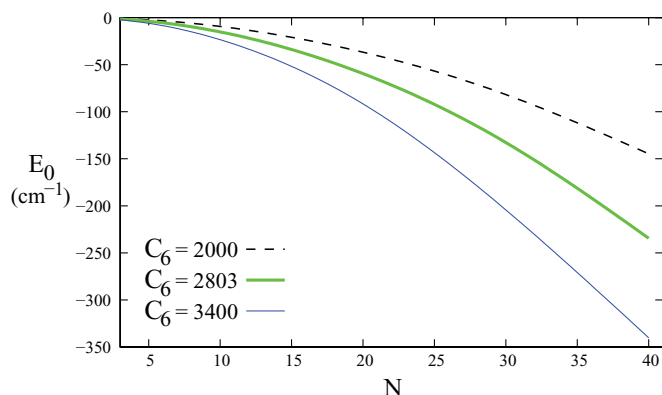


FIG. 5. Plot of ground state energy of Rb cluster with several indicated  $C_6$  parameters.

we obtain the same dimer scattering length (100 Bohr). We observed that for small particle number ( $N = 6$ ), the energy changes very little. However, for large cluster size, we observe a strong dominating role of the attractive tail of van der Waals interaction. It indicates that for such diffuse cluster, the shape independent approximation is valid only for very small size, it becomes invalid for larger cluster.

Although the average size of the clusters determines the diffuseness of the system, the pair distribution function  $P(r_{ij})$  is considered as a more effective quantity in the description of structural properties.  $P(r_{ij})$  determines the probability of finding the ( $ij$ ) pair of particles at a relative separation  $r_{ij}$ . The study of pair-correlation is important as the interatomic interaction plays a crucial role. When atoms try to form clusters due to the attractive part of van der Waal interaction, the short-range repulsion also comes into play. Due to the presence of the hard core part in interatomic interaction, atoms repel each other strongly at very small separation, which is of the order of the cut off radius  $r_c$  of the van der Waals interaction. Thus,  $P(r_{ij})$  vanishes for  $r_{ij}$  smaller than or of the order of  $r_c$ . It implies that the probability of finding the interacting pair at a separation  $\simeq r_c$  is zero. We calculate  $P(r_{ij})$  by

$$P(r_{ij}) = \int_{\tau''} |\Psi|^2 d\tau'', \quad (9)$$

where  $\Psi$  is the many-body wave function and the integral over the hypervolume  $\tau''$  excludes the integration over  $r_{ij}$ . After a lengthy calculation, we put it in a closed form as

$$P(r_{ij}) = \sqrt{2} \int_{-1}^1 \left(\frac{1-z}{2}\right)^\alpha \left(\zeta_0 \left(r_{ij} \sqrt{\frac{2}{1+z}}\right)\right)^2 \sum_{KK'} \left(\frac{h_K^{\alpha\beta}}{2^\alpha}\right)^{-1/2} \left(\frac{h_{K'}^{\alpha\beta}}{2^\alpha}\right)^{-1/2} (f_{Kl} f_{K'l})^{-1} \chi_{K0}(r) \chi_{K'0}(r) P_K^{\alpha\beta}(z) P_{K'}^{\alpha\beta}(z) dz, \quad (10)$$

where  $h_K^{\alpha\beta}$  is the norm of the Jacobi polynomial  $P_K^{\alpha\beta}(z)$  and

$$\int_0^\infty P(r_{ij}) r_{ij}^2 dr_{ij} = 1. \quad (11)$$

In Fig. 6, we plot  $P(r_{ij})$  for different particle number ( $N = 10, 20$ , and 30) for the dimer interaction.  $P(r_{ij})$  vanishes as

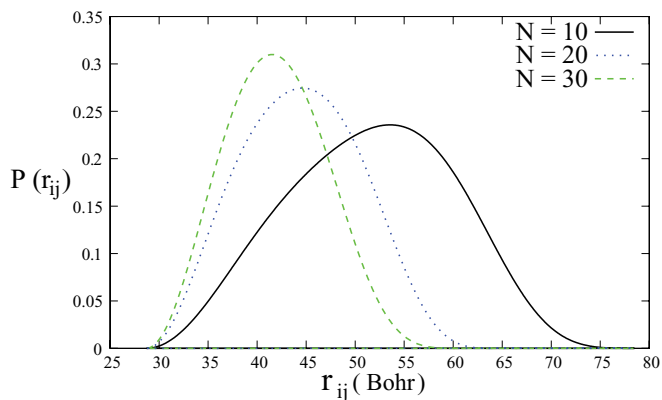


FIG. 6. Plot of normalised pair correlation function  $P(r_{ij})$  against pair separation  $r_{ij}$  for indicated cluster sizes ( $N$ ).

$r_{ij} \rightarrow r_c$  due to the presence of hard core repulsion of the van der Waals interaction as described above. The position of maximum in  $P(r_{ij})$  signifies that the probability of ( $ij$ ) pair to come closer is maximum at that separation. With increase in particle number the position of the maximum is shifted to smaller  $r_{ij}$  and the peak height becomes larger. This can be understood from the nature of  $\omega_0(r)$ . For  $N = 10$ , the depth of the lowest eigenpotential, as noted in Table I, is  $-15.369 \text{ cm}^{-1}$ . For a small number of atoms, the number of interacting pairs is small and net effective attractive interaction, coming from the interacting van der Waals pairs, is weak. Consequently, individual atoms are more spread out within the cluster and  $P(r_{ij})$  has a large width. It indicates that for weak interaction, the correlation length is large. Increasing  $N$  to 20, the number of interacting pair increases and the depth of the lowest eigenpotential increases to  $-59.774 \text{ cm}^{-1}$ . As the net attractive interaction sharply increases, atoms are drawn closer together and the correlation length decreases. Hence, the width (correlation length) of  $P(r_{ij})$  decreases, while its peak value increases. It indicates stronger pair correlation. As the width of the curve decreases further for  $N = 30$  with increase in the effective attractive interaction, the interacting pair is more localized. Shorter correlation length also induces stronger attraction. Hence, the system becomes more tightly bound with increasing  $N$ . This shows that if we go on increasing the particle number,  $P(r_{ij})$  will be sharply peaked at a small separation and the atoms will form strongly bound clusters.

### C. Energetics of $N$ -body clusters with tuned scattering length

Section III B was devoted to the study of structural properties of van der Waals clusters with Rb atoms at the fixed dimer scattering length. However, in the present state of experiments using Feshbach resonances, it is possible to tune the scattering length over a wide range, giving a control over the interatomic interaction. It makes us curious to study the properties of Rb clusters at other scattering lengths. For this purpose, we choose two other scattering lengths—one below (10 Bohr,  $r_c = 14.7532 \text{ \AA}$ ) and one above (2000 Bohr,  $r_c = 15.79526 \text{ \AA}$ ) the dimer scattering length (100 Bohr,  $r_c = 15.18 \text{ \AA}$ ).

For  $a_s = 10a_0$ , the system becomes more attractive and for  $a_s = 2000a_0$ , the system becomes less attractive compared to  $a_s = 100a_0$ . Since the binding energy for such a diffuse system comes from the interacting van der Waals pair, it is interesting to observe the stability of the cluster with such tuned scattering lengths. In Fig. 7, we plot the lowest effective potential for selected values of  $N$  and the chosen scattering lengths. For a fixed particle number and with increase in scattering length, we observe that the position of the minimum of the potential is slightly shifted towards larger  $r$ , but the well depth decreases more appreciably. Thus, an increase of positive  $a_s$  makes the net interaction less attractive. In a typical laboratory Bose-Einstein condensation produced within a trap, the interatomic separation is designed to be quite large, so that the two-body interaction is governed entirely by  $a_s$  and positive (negative)  $a_s$  represents repulsive (attractive) interaction. Hence, the condensate is not stable without the external trap. On the other hand, for van der Waals clusters (where no trap is needed), the interatomic separation is much less and binding is provided by the shorter range attractive part of the van der Waals potential. The effect of  $a_s$  produces a smaller perturbation due to its effect at larger (of order  $|a_s|$ , i.e.,  $\sim 100$  Bohr) separations. Positive  $a_s$  produces a small repulsive perturbation, as reflected in the behavior of  $\omega_0(r)$  in Fig. 7. On the contrary, He clusters are produced by actual He–He potential (say TTY potential<sup>26</sup>) and their structure and energetics are markedly different from those of van der Waals clusters. Figure 7 also shows some plateau-like regions, which are similar to those found in the earlier study of Ne and Ar clusters.<sup>18</sup> These represent fragmentation channels of the cluster for large hyper-radius. In our present method, we cannot calculate the geometry of the clusters with more than three atoms. However, similar features for a larger systems may signify the changes in geometry as the hyper-radius reaches the plateau value, increasing from the value at which  $\omega_0(r)$  has a minimum.

In Fig. 8, we plot energies of the ground state and the first excited state as functions of  $N$  for the chosen scattering lengths. All the states become more strongly bound with increase in cluster size  $N$  for a fixed scattering length. For a fixed  $N$ , all the excited states are maximally bound for  $a_s = 10a_0$ , and binding weakens as  $a_s$  increases. These are in agreement with our remarks in the previous paragraph.

We now investigate correlation between energies of two consecutive clusters differing in size by one atom. This type of study is essential to describe the universal properties of such diffuse system. There are many important works in literature,<sup>3,18,27–29</sup> which study the universal properties of Efimov states of ultracold atoms. While the universal behaviour of trimer is well known,<sup>3</sup> it is not clear for large system. In nuclear physics, there are a number of studies focused on the Tjon line, which refers to an approximate linear correlation between the energy of four and three nuclear systems. Later, the conception of Tjon line was extended to establish the correlation between trimer and tetramer energies of weakly bound cluster and a linear relationship between the energies of two clusters differing in size by one atom is predicted as  $E^{(N+1)} = B_N + C_N E^{(N)}$ ,<sup>5</sup> where  $E^{(N)}$  is the ground state energy of the cluster of  $N$  atoms. To establish the universality of Rb



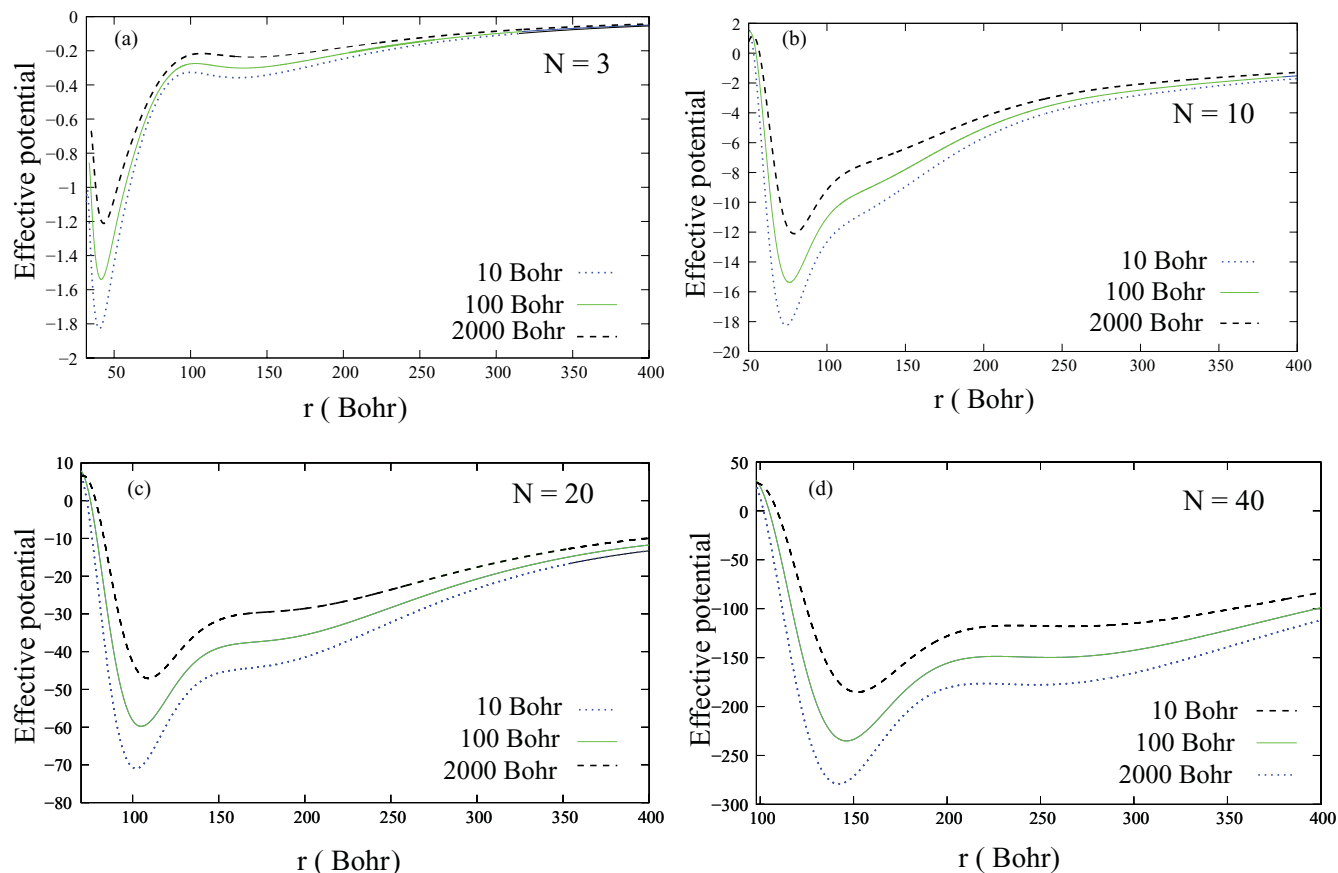


FIG. 7. Plot of effective potential  $\omega_0(r)$  (in  $\text{cm}^{-1}$ ) as functions of hyper-radius  $r$  (in Bohr) for clusters containing  $N = 3, 10, 20,$  and  $40$  Rb atoms with  $a_{sc} = 10, 100,$  and  $2000$  Bohr.

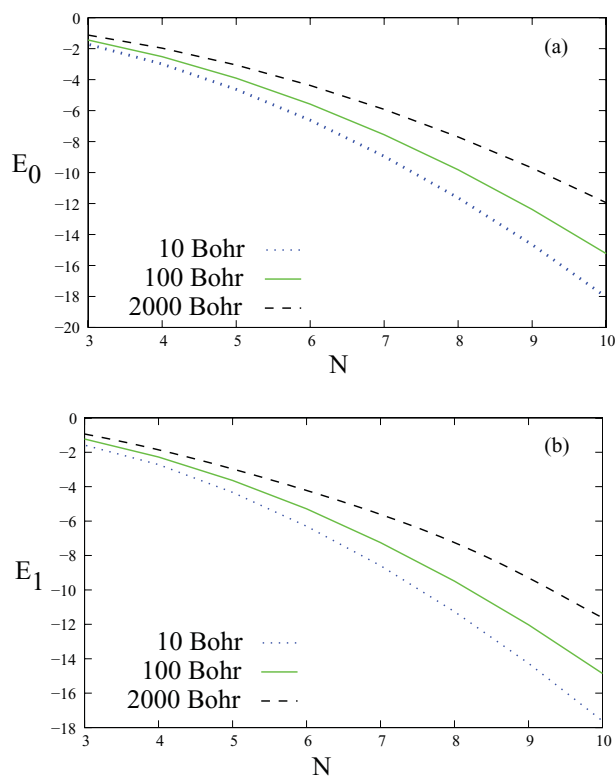


FIG. 8. Energies (in  $\text{cm}^{-1}$ ) of ground state ( $E_0$ ) and first excited state ( $E_1$ ) of Rb cluster as functions of cluster size  $N$  for the chosen scattering lengths, as indicated in the figure.

diffuse cluster, we calculate the ground state energy of dimer ( $E^{(2)}$ ), trimer ( $E^{(3)}$ ), and tetramer ( $E^{(4)}$ ) with variable scattering length and plot in Fig. 9. We plot the ratio between ground state energy  $E^{(4)}$  and  $E^{(2)}$  as a function of ratio between the ground state energies  $E^{(3)}$  and  $E^{(2)}$ . Thus, we scale the trimer and tetramer energies by the dimer energy. The dependence of  $\frac{E^{(4)}}{E^{(2)}}$  on  $\frac{E^{(3)}}{E^{(2)}}$  is quite well described by a two parameter fit of the form  $\frac{E^{(4)}}{E^{(2)}} = B_3 + C_3 \frac{E^{(3)}}{E^{(2)}}$ . It confirms the existence of Tjon line. Next, to investigate the correlation between ground

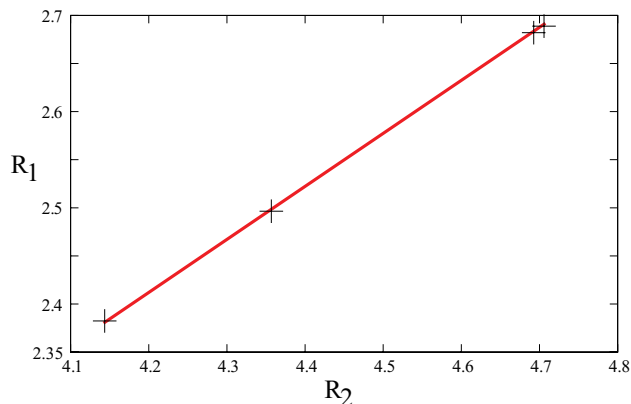


FIG. 9. Plus sign shows the energy ratio,  $R_1 = \frac{E^{(4)}}{E^{(2)}}$  as a function of energy ratio,  $R_2 = \frac{E^{(3)}}{E^{(2)}}$ . Solid line is our two parameter fit. Details are in the text.

state energy of  $(N + 1)$  atom  $N$  atom and  $(N - 1)$  atom clusters, we find an approximately linear relationship, which fits as  $\frac{E^{(N+1)}}{E^{(N-1)}} = B_N + C_N \frac{E^{(N)}}{E^{(N-1)}}$ . We plot the energy ratios  $\frac{E^{(N+1)}}{E^{(N-1)}}$  as a function of  $\frac{E^{(N)}}{E^{(N-1)}}$  for  $N = 4 - 9$  in Fig. 10. From the above-mentioned linear fit of the above form, we calculate the fitting parameters  $B_N$  and  $C_N$  and those values are presented in Table IV. Our observation nicely demonstrates the generalised Tjon lines, which refers to the approximate linear dependence of the energy ratio of the clusters.

Next the study of atom loss due to the three-body recombination process is also an important area of discussions as it is highly related with the stability of cluster. As seen from the effective potential ( $\omega_0(r)$ ) for different cluster size, it has a long tail, which extends up to few hundreds Bohr. Thus,

TABLE IV. Fitting parameters  $B_N$  and  $C_N$  for  $N = 4 - 9$ .

$N$	$B_N$	$C_N$
4	-1.0457	2.1485
5	-0.9955	2.0812
6	-0.9677	2.0300
7	-0.8288	1.9116
8	-0.6578	1.7636
9	-0.5002	1.6270

the stable cluster formed in the deep negative well in the left side will not suffer any quantum tunnelling. However, as the size of the well is quite narrow and deep, the recombination process is important, which causes the loss of atoms. We

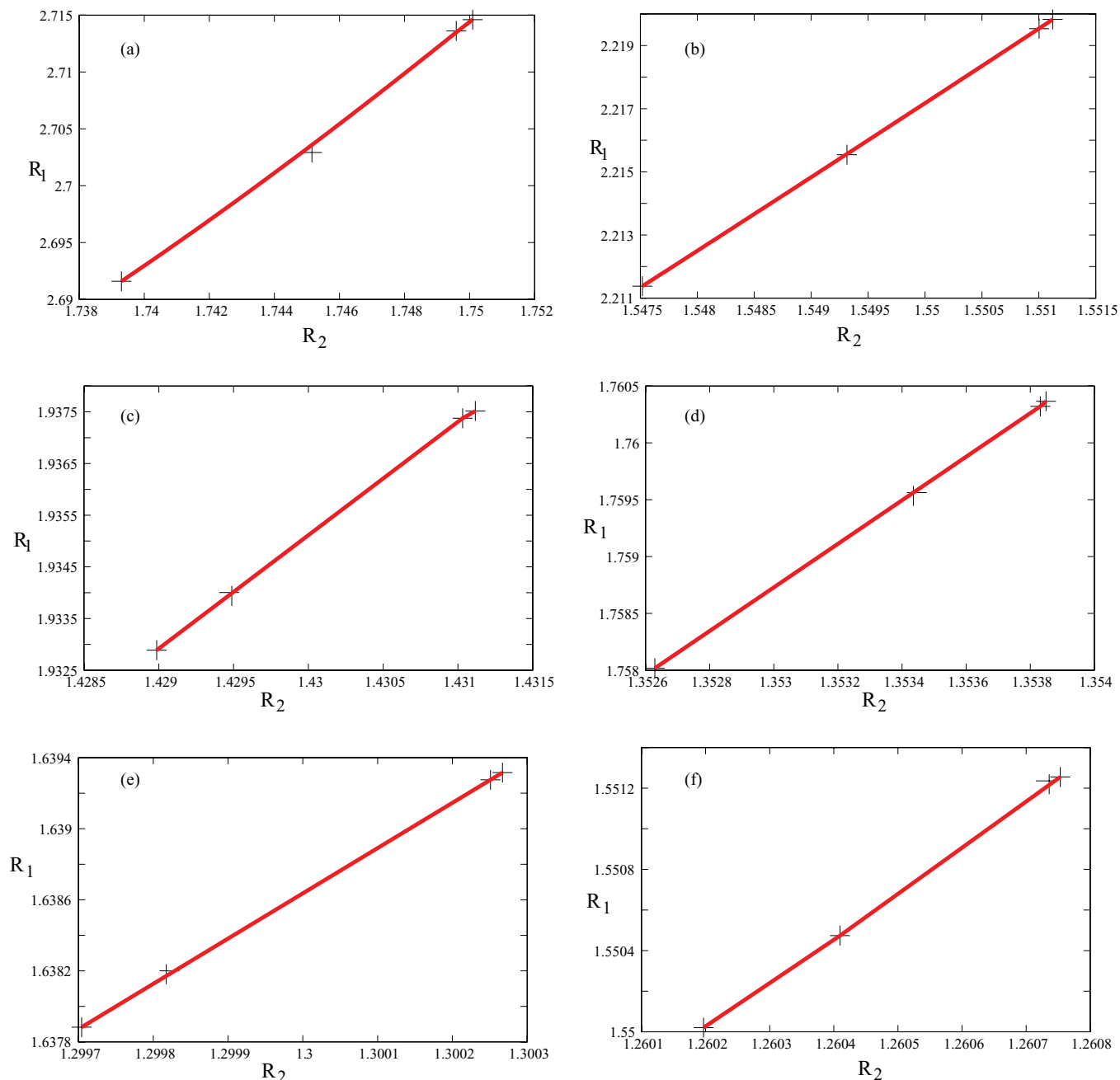


FIG. 10. Plus sign shows the energy ratio,  $R_1 = \frac{E^{(N+1)}}{E^{(N-1)}}$ , as a function of energy ratio,  $R_2 = \frac{E^{(N)}}{E^{(N-1)}}$ , for (a)  $N = 4$ , (b)  $N = 5$ , (c)  $N = 6$ , (d)  $N = 7$ , (e)  $N = 8$ , (f)  $N = 9$ . Solid line is our two parameter fit. Details are in the text.

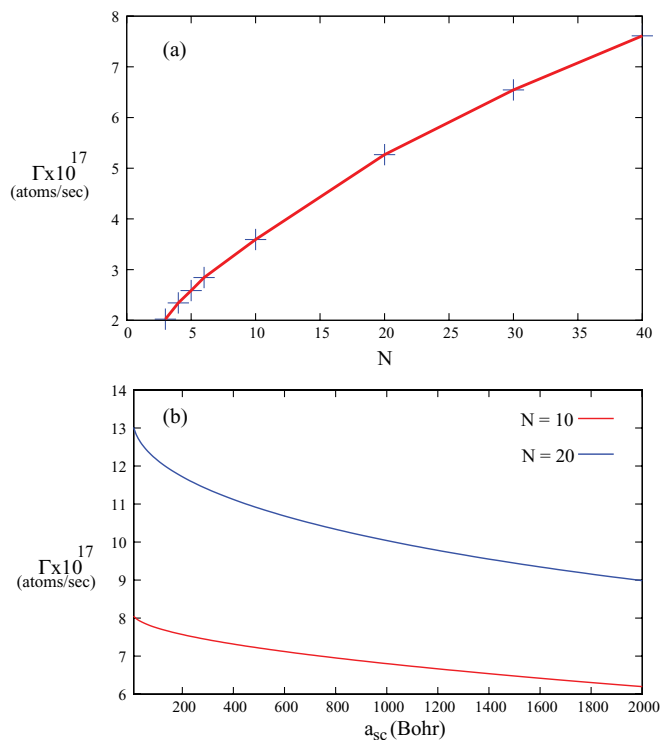


FIG. 11. Loss rate due to three-body collisions, (a) as a function of cluster size for dimer scattering length; (b) as a function of scattering length for two fixed sizes of cluster as indicated in the figure.

calculate the loss rate due to three-body recombination as

$$\Gamma_{3-body} = L_{3-body} \int |\Psi(\vec{r})|^6 d^3r, \quad (12)$$

where  $\Psi(\vec{r})$  is the normalised cluster wave function and  $L_{3-body}$  is the three-body recombination loss rate coefficient for *Rb* atoms, whose value is  $L_{3-body} = 4.0 \times 10^{18} \text{ \AA}^6 \text{ s}^{-1}$  (Ref. 7). The calculated value for  $\Gamma_{3-body}$  for dimer scattering length is plotted in Fig. 11(a), as a function of cluster size. It shows that for larger cluster size, the loss-rate is quite significant as the many-body effective potential becomes deeper and deeper with increase in cluster size. In Fig. 11(b), we plot the loss-rate as a function of tuned scattering length for a different choice of cluster size. The behaviour of  $\Gamma$  as a function of  $N$  is quite understandable from the behaviour of  $\omega_0(r)$ . For large scattering length, as the minimum of  $\omega_0(r)$  sharply shifts upward (as the system becomes less attractive), the loss rate sharply falls.

#### IV. SUMMARY AND CONCLUSIONS

We have investigated the energetics and structure of diffuse *Rb* clusters containing up to  $N = 40$  atoms by using the potential harmonics expansion method in which a subset (including two-body correlation only) of hyperspherical harmonics basis functions has been used to expand each Faddeev component. The interatomic potential is chosen to be the van der Waals potential, with the short-range repulsion represented by a hard core, whose radius is adjusted to reproduce the *Rb* dimer scattering length. As a test of the reliability of this potential, we also used the realistic Lennard-Jones poten-

tial, whose  $C_{12}$  coefficient was adjusted to give the appropriate scattering length. Calculated ground state energies differ by a small amount, showing that our choice of van der Waals potential is appropriate. The effective potential in the hyper-radial space is obtained by solving the hyperangular motion in the hyperspherical adiabatic approximation. This potential is used to calculate energetics and various structural properties of different cluster size  $N$ . The study of such a cluster is very important for several reasons. Although rare gas clusters (like He, Ne, Ar clusters) are already well studied, the study of *Rb*-clusters has not been undertaken so far. Unlike the rare gas clusters, *Rb* cluster is diffuse. Although a dilute gas of trapped *Rb* atoms is already studied in mean-field and many-body theories, bound states of trapless *Rb* atoms are not studied yet. This is specially interesting, as in the present-day experiments, it is possible to create large weakly bound clusters by utilizing Feshbach resonances. Thus, it is important to investigate the possibility of formation of van der Waals clusters and to study their stability. Our present calculation gives qualitative as well as quantitative results, which will help to analyse experimental findings for such trapless clusters in the near future. The comparison with other well studied clusters is also presented for better understanding. The methodology used in the present calculation is valid for quite a large number of atoms in the cluster, so direct verification with the experiments is possible. We find that for  $N \leq 40$  atoms, the system is very diffuse. Due to small kinetic energy, the interacting pair does not come too close together. Hence, no short-range correlation function due to the repulsive core was needed with the PH basis. This is in contrast with light He clusters, where short-range correlation is important. However, larger clusters with negative scattering length may require the use of correlated potential harmonics basis, as the system (especially for the high lying excited states) is likely to develop short-range correlations. We have already applied this basis to light He clusters and the calculated results are in good agreement with the DMC results. We have also investigated the effects of tuning the positive scattering length both above and below the dimer value. It is found that its effect is a small perturbation of the main attraction provided by the short range ( $\sim 30$  Bohr) part of the van der Waals interaction. Thus, the main binding comes from the attractive part of the van der Waals potential giving rise to relatively well bound but well extended van der Waals clusters. We also test the validity of shape-independent approximation in the calculation of ground state energy for different cluster size. We show that the trimer and tetramer energies scaled by the corresponding dimer energies fall on the Tjon line. For large clusters, differing in size by one atom, also approximately satisfy a linear relation in the energy ratio, which indicates the generalised Tjon line for such diffuse clusters. We also calculate the decay rate due to three-body recombination. This theoretical study is expected to stimulate the experimental investigation of trapless light Rubidium clusters.

#### ACKNOWLEDGMENTS

This work has been partially supported by the FAPESP (Brazil), CNPq (Brazil), Department of Science and Technol-

ogy (DST, India), and Department of Atomic Energy (DAE, India). T.K.D. acknowledges the University Grants Commission (UGC, India) for the Emeritus Fellowship program. B.C. wishes to thank the FAPESP (Brazil) for providing financial assistance for her visit to the Universidade de São Paulo, Brazil, where a part of this work was done.

- <sup>1</sup>T. K. Lim, S. Nakaichi, Y. Akaishi, and H. Tanaha, *Phys. Rev. A* **22**, 28 (1980).
- <sup>2</sup>L. Platter, H.-W. Hammer, Ulf-G. Meißner, *Phys. Rev. A* **70**, 052101 (2004).
- <sup>3</sup>E. Braatin and H.-W. Hammer, *Phys. Rep.* **428**, 259 (2006).
- <sup>4</sup>D. Blume, B. D. Esry, C. H. Greene, N. N. Klausen, and G. J. Hanna, *Phys. Rev. Lett.* **89**, 163402 (2002).
- <sup>5</sup>G. J. Hanna and D. Blume, *Phys. Rev. A* **74**, 063604 (2006).
- <sup>6</sup>F. Dalfovo, S. Giorgini, L. P. Pitaevskii, and S. Stringari, *Rev. Mod. Phys.* **71**, 463 (1999).
- <sup>7</sup>C. J. Pethick and H. Smith, *Bose-Einstein Condensation in Dilute Gases* (Cambridge University Press, Cambridge, 2002).
- <sup>8</sup>J. L. Roberts *et al.*, *Phys. Rev. Lett.* **86**, 4211 (2001); **81**, 5109 (1998).
- <sup>9</sup>E. Tiesinga, B. J. Verhaar, and H. T. C. Stoof, *Phys. Rev. A* **47**, 4114 (1993).
- <sup>10</sup>E. A. Donley, N. R. Clauseen, S. T. Thompson, and C. E. Wieman, *Nature (London)* **417**, 529 (2002).
- <sup>11</sup>C. A. Regal, M. Greiner, and D. S. Jin, *Phys. Rev. Lett.* **92**, 040403 (2004).
- <sup>12</sup>M. W. Zwierlein, C. A. Stan, C. H. Schunck, S. M. F. Raupach, A. J. Kerman, and W. Ketterle, *Phys. Rev. Lett.* **92**, 120403 (2004).
- <sup>13</sup>B. D. Esry, and C. H. Greene, *Phys. Rev. A* **60**, 1451 (1999); T. K. Das, R. Chattopadhyay, and P. K. Mukherjee, *Phys. Rev. A* **50**, 3521 (1994); T. K. Das, H. T. Coelho, and M. Fabre de la Ripelle, *Phys. Rev. C* **26**, 2288 (1982); M. Breiner and M. Fabre de la Ripelle, *Lett. Nuovo Cimento Soc. Ital. Fis.* **1**, 584 (1971).
- <sup>14</sup>T. K. Das and B. Chakrabarti, *Phys. Rev. A* **70**, 063601 (2004).
- <sup>15</sup>T. K. Das, S. Canuto, A. Kundu, and B. Chakrabarti, *Phys. Rev. A* **75**, 042705 (2007).
- <sup>16</sup>T. K. Das, B. Chakrabarti, and S. Canuto, *J. Chem. Phys.* **134**, 164106 (2011).
- <sup>17</sup>T. K. Das, A. Kundu, S. Canuto, and B. Chakrabarti, *Phys. Lett. A* **373**, 258 (2009).
- <sup>18</sup>D. Blume and C. H. Greene, *J. Chem. Phys.* **113**, 4242 (2000).
- <sup>19</sup>M. Fabre de la Ripelle, *Ann. Phys. (N.Y.)* **147**, 281 (1983).
- <sup>20</sup>J. L. Ballot and Fabre de la Ripelle, *Ann. Phys. (N.Y.)* **127**, 62 (1980).
- <sup>21</sup>R. M. Adams and S. A. Sofianos, *Phys. Rev. A* **82**, 053635 (2010).
- <sup>22</sup>T. K. Das, H. T. Coelho, and M. Fabre de la Ripelle, *Phys. Rev. C* **26**, 2281 (1982).
- <sup>23</sup>V. P. Brito, H. T. Coelho, and T. K. Das, *Phys. Rev. A* **40**, 3346 (1989); S. K. Adhikari, V. P. Brito, H. T. Coelho, and T. K. Das, *Nuo. Cim. B* **107**, 77 (1992).
- <sup>24</sup>B. Chakrabarti and T. K. Das, *Phys. Rev. A* **78**, 063608 (2008).
- <sup>25</sup>D. Blume and C. H. Greene, *J. Chem. Phys.* **112**, 8053 (2000).
- <sup>26</sup>K. T. Tang, J. P. Toennies, and C. L. Yiu, *Phys. Rev. Lett.* **74**, 1546 (1995).
- <sup>27</sup>P. F. Bedaque, H.-W. Hammer, and U. van Kolck, *Phys. Rev. Lett.* **82**, 463 (1999).
- <sup>28</sup>P. F. Bedaque, H.-W. Hammer, and U. van Kolck, *Nucl. Phys. A* **646**, 444 (1999).
- <sup>29</sup>M. T. Yamashita, L. Tomio, A. Delfino, and T. Frederico, *Europhys. Lett.* **75**, 555 (2006).